

Model-Based Safe Policy Search from Signal Temporal Logic Specifications Using Recurrent Neural Networks

Wenliang Liu and Calin Belta

Abstract—We propose a policy search approach to learn controllers from specifications given as Signal Temporal Logic (STL) formulae. The system model is unknown, and it is learned together with the control policy. The model is implemented as a feedforward neural network (FNN). To capture the history dependency of the STL specification, we use a recurrent neural network (RNN) to implement the control policy. In contrast to prevalent model-free methods, the learning approach proposed here takes advantage of the learned model and is more efficient. We use control barrier functions (CBFs) with the learned model to improve the safety of the system. We validate our algorithm via simulations. The results show that our approach can satisfy the given specification within very few system runs, and therefore it has the potential to be used for on-line control.

I. INTRODUCTION

Temporal logics, such as Linear Temporal Logic (LTL) and Computation Tree Logic (CTL), have been traditionally used as specification languages for digital circuits and computer programs [1]. Due to their expressivity, the availability of tools for verification and synthesis, and recent advances in abstraction techniques for dynamical systems, temporal logics have been increasing used as specification languages in robotics, biology, and autonomous driving applications.

In this paper, we focus on Signal Temporal Logic (STL), which was introduced in [2] to monitor temporal properties of real-valued signals. STL is equipped with quantitative semantics, known as robustness, which assigns a real value to measure how much a signal satisfies a formula [3]. Using robustness, controlling a system from an STL specification can be formulated as an optimization problem. The STL robustness was used as a constraint in the optimization problems formulated in [4] and [5]. This optimization problem is solved using Mixed Integer Programming (MIP) in a Model Predictive Control (MPC) manner. In [6], [7], [8], [9], [10] smooth approximations of STL robustness were proposed to enable the use of gradient-based methods. In these works, the STL robustness is directly used as an objective function to be maximized over control signals. However, both MIP and gradient-based methods are computationally expensive, especially for high dimensional systems and long-horizon planning, which prevents real-time implementation.

Neural Network (NN) - based controllers have been proposed to address the computational complexity of the methods described above. NNs can be trained offline and

executed online, which enables real-time implementation. In [11], the control policy is parameterized as a Feedforward Neural Network (FNN). Its input is the current system state and the output is the control that maximizes the STL robustness. FNNs are memoryless controllers. However, STL satisfaction is, in general, *history-dependent*. For instance, if a specification requires an agent to visit region A and then region B, the agent needs to know whether it has already visited region A in order to decide which region it should go at the current time. A Recurrent Neural Network (RNN) controller, which has memory, was proposed in [12] to satisfy STL specifications. The RNN was trained on a dataset containing trajectories generated from optimization methods, which is again computationally expensive. Besides, all the above approaches assume the system dynamics are known, which is typically not the case in practice.

Reinforcement Learning (RL) can solve control problems for systems with unknown dynamics. After the policy is learned, it can be executed in real-time. Recently, RL approaches have been investigated to synthesize controllers satisfying STL specifications. The advantage of combining RL and STL is that the STL robustness can be used as RL rewards, which avoids reward hacking [13]. The authors of [14] and [15] used Q-learning to learn control policies that maximize the robustness of STL fragments, which only applies to discrete state and control spaces. A similar idea was used in [16], where deep Q-learning was applied to continuous state and control space. These methods restrict the specification to be a fragment of STL. Path integral was used for learning control policies from Truncated Linear Temporal Logic (TLTL) [17], [18] and STL [19]. The authors of [20] translated a TLTL specification into a finite-state automaton and used proximal policy optimization to train an FNN controller. These methods are completely model-free, and are therefore data inefficient, i.e., they require a large number of trials to learn the policy. Hence, they cannot be used in applications where many executions take a lot of time, and wear out or even damage the systems.

Model-based policy search methods (e.g., [21], [22]) learn a dynamic model of the system and use it to guide policy search. They are more efficient than model-free methods. The authors of [23] trained an FNN to predict the system transitions and used MPC with the learned model to find the controller that maximizes STL robustness. The MPC problem was solved using an evolutionary strategy, which is slow and cannot be implemented in real time. The authors of [11] also utilized the system model when training the FNN controller from STL, but they assumed that the model was known.

This work was partially supported by the National Science Foundation under grants IIS-2024606 and IIS-1723995.

The authors are with Boston University, Boston, MA, USA
wliu97@bu.edu, cbelta@bu.edu

In this paper, we propose a model-based policy search method that learns both the system model and the control policy from an STL specification. Taking advantage of the learned model, the policy can be learned from very few trials (system executions). We use a probabilistic system model to reduce model bias [21]. The model is implemented as an FNN with dropout, which is an approximation of a Bayesian neural network [24]. The control policy is an RNN, which outputs the control depending on current state and past states, and can therefore satisfy general STL specifications. We extend the Lagrange multiplier method from [11] to train the RNN controller. The gradient of the STL robustness is computed automatically and analytically, leveraging the technique from [25]. After training, the RNN controller can be executed very fast, which enables real time implementation.

Another critical concern for RL is safety: unsafe states should never be reached during training and testing of the controller. Control Barrier Functions (CBF) [26] have been proposed to obtain safe control actions. In [20], CBFs is incorporated with formal methods to guarantee the safety of RL. Typically, using CBF requires the system dynamics to be known. In this paper, the system model is unknown, so we propose a method that applies CBF to the learned probabilistic model, which takes into account the model uncertainty in order to improve safety performance.

II. NOTATIONS AND PRELIMINARIES

We consider a discrete-time dynamical system:

$$x_{t+1} = f(x_t, u_t), \quad t = 0, 1, \dots \quad (1)$$

where $x_t \in \mathcal{X} \subseteq \mathbb{R}^n$ is the system state, $u_t \in \mathcal{U} \subseteq \mathbb{R}^m$ is the control input at time t , and $f : \mathcal{X} \times \mathcal{U} \rightarrow \mathcal{X}$ is the dynamics. Let $x_{t_1:t_2}$ denote the partial state trajectory $x_{t_1}, x_{t_1+1}, \dots, x_{t_2}$ with $t_2 > t_1$.

A. Signal Temporal Logic (STL)

An n -dimensional real-valued signal is denoted as $X = x_0 x_1 \dots$, where $x_t \in \mathbb{R}^n$, $t \in \mathbb{Z}_{\geq 0}$. The STL syntax [2] is defined and interpreted over X :

$$\varphi := \top \mid \mu \mid \neg \varphi \mid \varphi_1 \wedge \varphi_2 \mid \varphi_1 \mathbf{U}_I \varphi_2, \quad (2)$$

where $\varphi, \varphi_1, \varphi_2$ are STL formulae, \top is the Boolean constant *True*, and \neg and \wedge are the Boolean *negation* and *conjunction* operators, respectively. μ is a *predicate* over signals of the form $\mu := l(x_t) \geq 0$, where $l : \mathbb{R}^n \rightarrow \mathbb{R}$ is a Lipschitz continuous function. $I = [a, b] = \{t \in \mathbb{Z}_{\geq 0} \mid a \leq t \leq b; a, b \in \mathbb{Z}_{\geq 0}\}$ denotes a bounded time interval and \mathbf{U} is the temporal *until* operator. $\varphi_1 \mathbf{U}_I \varphi_2$ states that “ φ_2 becomes true at some time point within I and φ_1 must be always true prior to that.” The Boolean constant \perp (*False*) and *disjunction* \vee can be defined from \top , \neg , and \wedge in the usual way. Additional temporal operators can also be defined, e.g., *eventually* and *always* are defined as $\mathbf{F}_I \varphi := \top \mathbf{U}_I \varphi$ and $\mathbf{G}_I \varphi := \neg \mathbf{F}_I \neg \varphi$, respectively. $\mathbf{F}_I \varphi$ is satisfied if “ φ becomes *True* at some time in I ” while $\mathbf{G}_I \varphi$ is satisfied if “ φ is *True* at all times in I ”.

The STL *qualitative semantics* [2] determines *whether* a signal X satisfies a formula φ (written as $S \models \varphi$) or not

(written as $S \not\models \varphi$). Its *quantitative semantics*, or *robustness*, assigns a real value to measure *how much* a signal satisfies φ . Multiple functionals have been proposed to capture the STL robustness [3], [7], [9], [10]. In this paper, we use the robustness function proposed in [9] which is a *sound* score, i.e., a strictly positive robustness indicates satisfaction of the formula, and a strictly negative robustness indicates violation. As opposed to the traditional robustness [3], the robustness in [9] is differentiable so it is suitable for gradient-based optimization methods. We denote the robustness of φ at time t with respect to signal X by $\rho(\varphi, X, t)$. For brevity, we denote $\rho(\varphi, X, 0)$ by $\rho(\varphi, X)$. The time horizon of an STL formula φ denoted by $\text{hrz}(\varphi)$ is the closest time point in the future for which signal values are needed to compute the robustness at the current time [27].

B. Recurrent Neural Network (RNN) Controller

Due to the *history-dependence* property of STL, a feedback controller for system (1) required to satisfy an STL formula over its state at time t , should be a function of the current state and all the history states, i.e., $u_t = \pi(x_{0:t})$. In this paper, we will learn a controller in the form of an RNN [28], which can be formulated as follows:

$$\begin{aligned} \mathbf{h}_t &= \mathcal{R}(x_t, \mathbf{h}_{t-1}, W_1), \\ u_t &= \mathcal{N}(\mathbf{h}_t, W_2), \end{aligned} \quad (3)$$

where \mathbf{h}_t is the RNN hidden state, $t = 0, 1, \dots, T-1$ (T is the final time of interest). At time t , the input of the RNN is the current system state x_t , and the output is the control u_t . \mathcal{R} represents some fully connected layers with parameters W_1 , which update the hidden state based on the input and the previous hidden state. \mathcal{N} represents some layers with parameters W_2 , which predict the output based on the hidden state. The output layer is applied a hyperbolic tangent function to satisfy the control constraint $u \in \mathcal{U}$ as in [11]. The hidden state \mathbf{h}_t encodes all the previous inputs. \mathbf{h}_{-1} is a zero vector.

C. Discrete Time Control Barrier Function

Consider system (1) and let $b : \mathbb{R}^n \rightarrow \mathbb{R}$. The set $\mathcal{C} = \{x \in \mathbb{R}^n \mid b(x) \geq 0\}$ is (forward) *invariant* for system (1) if all its trajectories remain in \mathcal{C} for all times, if they originate in \mathcal{C} . Function b is a (discrete-time, exponential) *Control Barrier Function* (CBF) [29] for system (1) if there exists $\alpha \in [0, 1]$, and for each x_t there exists $u_t \in \mathcal{U}$ such that:

$$\begin{aligned} b(x_0) &\geq 0 \\ b(x_{t+1}) + (\alpha - 1)b(x_t) &\geq 0, \quad \forall t \in \mathbb{Z}_{\geq 0}, \end{aligned} \quad (4)$$

where x_{t+1} , x_t , and u_t are related by (1). The set \mathcal{C} is invariant for system (1) if there exists a CBF b as in (4) [29]. This invariance property is usually referred to as *safety*. In other words, the system is safe if it stays inside the set \mathcal{C} .

III. PROBLEM STATEMENT AND APPROACH

Consider system (1) with unknown dynamics f and fully observable state. We assume that the initial state x_0 is randomly located in a set $\mathcal{X}_0 \subseteq \mathcal{X}$ with the probability

density function $p : \mathcal{X}_0 \rightarrow \mathbb{R}$. Given an STL formula φ with predicates interpreted over x , and given a finite time horizon $T \geq \text{hrz}(\varphi)$ (for simplicity we assume that $T = \text{hrz}(\varphi)$), our goal is to find a control policy $u_t = \pi(x_{0:t})$, $t = 0, \dots, T-1$ that makes trajectories $x_{0:T}$ starting from \mathcal{X}_0 satisfy φ . Since the robustness is sound, we can use it as a reward, and find a controller that maximize its expectation.

In this paper we use a parameterized policy, which is implemented by an RNN. The control u_t is computed by using (3) recursively. We denote $u_t = \pi(x_{0:t}; W)$, where $W = (W_1, W_2)$ captures the RNN parameters. We now formally state the STL control synthesis problem as follows:

Problem 1. Given system (1) with unknown dynamics f , fully observable state, initial state x_0 with distribution $p : \mathcal{X}_0 \rightarrow \mathbb{R}$, and given an STL formula φ over x with $T = \text{hrz}(\varphi)$, find the optimal policy parameters W^* that maximize the expected STL robustness, i.e.,

$$\begin{aligned} W^* &= \arg \max_W E_{p(x_0)}[\rho(\varphi, x_{0:T})] \\ \text{s.t. } x_{t+1} &= f(x_t, \pi(x_{0:t}; W)), \quad t = 0, 1, \dots, T-1. \end{aligned} \quad (5)$$

Since the system model f is unknown, Pb. 1 cannot be solved directly. We first execute the system with random controls and collect the resulting system state transitions to form a dataset. We train an FNN model (different from the RNN controller) on this dataset to approximate the model f . Then we solve Pb. 1 using the learned model to improve the control policy. We alternately improve the system model using the data collected by applying the new policy, and improve the policy using the new model until convergence. CBF is applied at each time the system is executed to improve safety except for generating the initial dataset, where safety is ensured by checking the distance to the unsafe area. The overall model-based policy search framework is shown in Fig. 1. The technical details are presented in Sec. IV.

Model-based learning is much more data-efficient than model-free RL methods, i.e., it requires fewer trials to learn the policy. Alternately training the system model and the control policy benefits both. With a better policy, more states that the system may reach in order to finish the task can be explored, which results in a better model. On the other hand, with a more precise model, the policy can be better tuned.

IV. MODEL-BASED POLICY SEARCH

In this section, we introduce the model-based policy search approach for satisfying STL specifications. The model learning, the control policy improvement, and the overall model-based policy search algorithms are presented in Secs. IV-A, IV-B and IV-C, respectively.

A. System Model Learning

We use a probabilistic model implemented by a feedforward neural network (FNN) \mathcal{F} with dropout to predict the system state difference $\Delta_t = x_{t+1} - x_t$ given the current state x_t and the control input u_t :

$$\hat{\Delta}_t = \mathcal{F}(x_t, u_t; W_0, Z_0), \quad (6)$$

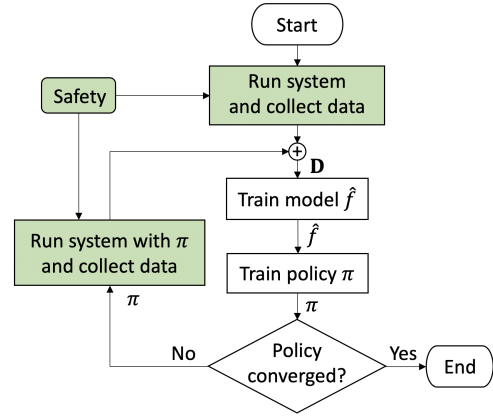


Fig. 1: Our overall approach to Problem 1: We first generate an initial dataset \mathbf{D} , and then we train the system model and the control policy alternately. Safety is guaranteed when running the system. The iterative procedure terminates when the policy converges.

where W_0 are FNN parameters, Z_0 is a random dropout mask that randomly deactivates the nodes in the dropout layers with probability p_d . As an approximation of a Bayesian Neural Network, an FNN with dropout can not only reduce model bias (detailed in Sec. IV-B) but also represent model uncertainty via moment-matching [24]. To do this, we evaluate the FNN with the input (x_t, u_t) and randomly sampled dropout masks $Z_0^1, \dots, Z_0^{N_z}$, and obtain the outputs $\hat{\Delta}_t^1, \dots, \hat{\Delta}_t^{N_z}$. The model uncertainty at (x_t, u_t) is represented by the covariance Σ_t of the outputs. For simplicity, we assume a constant covariance Σ , which is the mean of a set of covariances evaluated at randomly sampled FNN inputs. The FNN can be easily transformed into a deterministic form by applying a mask Z_{det} that activates all nodes and scaling the outputs of dropout layers by a factor of $1 - p_d$.

To learn the model, we need to execute the system and record the system transitions. Safety should be considered in this process. When first running the system, we have no knowledge about the dynamics, so we simply check if the state is too close to the unsafe area at each time. If the distance is less than a given threshold, we stop the system. Specifically, we sample N_0 random initial states $\{x_0^1, \dots, x_0^{N_0}\}$ from the probability distribution p . From each initial state, we apply random controls $u_t \sim \text{Uniform}(\mathcal{U})$ until we reach the time horizon T or the system is stopped because it is too close to the unsafe area. We collect all the system transitions $((x_t^i, u_t^i), \Delta_t^i)$ with $i = 1, \dots, N_0$ at all times t to create the initial dataset \mathbf{D} . Then the FNN is trained on \mathbf{D} to minimize the loss C , which is defined as:

$$C = \sum_{\mathbf{D}} \sum_{t=0}^{T-1} \|\Delta_t - \mathcal{F}(x_t, u_t; W_0, Z_0)\|^2. \quad (7)$$

After training, the FNN parameters are denoted by W_0^* .

Each time after the control policy is improved using the current model, we apply the new policy and collect more system transition data. When doing this, we use a CBF with the learned model to improve safety. Here we transform the

FNN model (6) into the form:

$$\hat{\Delta}_t = \mathcal{F}(x_t, u_t; W_0, Z_{det}) + \delta, \quad (8)$$

where δ is a zero-mean noise with covariance Σ . The noise δ introduces an error ϵ into $b(x_{t+1})$ in (4):

$$b(x_{t+1}) = b(x_t + \mathcal{F}(x_t, u_t; W_0, Z_{det})) + \epsilon. \quad (9)$$

We use the first order derivative to approximate the error:

$$\epsilon = \left. \frac{\partial b}{\partial x} \right|_{x=x_t + \mathcal{F}(x_t, u_t; W_0, Z_{det})} \cdot \delta. \quad (10)$$

For brevity, in what follows, we omit the point that the derivative is evaluated at. The error ϵ is a zero-mean random variable with variance σ^2 , which is given by:

$$\sigma^2 = \left(\frac{\partial b}{\partial x} \right) \Sigma \left(\frac{\partial b}{\partial x} \right)^\top. \quad (11)$$

By Choosing a lower limit of the error ϵ in (9) to compute $b(x_{t+1})$, we can guarantee the safety for all $\epsilon \geq -2\sigma$. At time t and state x_t , we obtain the safe control u_t^s as:

$$u_t^s = \arg \min_u \|u - \pi(x_{0:t}, W)\|^2$$

$$\text{s.t. } b(x_t + \mathcal{F}(x_t, u_t; W_0, Z_{det})) + (\alpha - 1)b(x_t) \geq 2\sigma, \quad (12)$$

where $\alpha \in [0, 1]$. We solve this optimization problem by using Sequential Quadratic Programming (SQP) [30].

Similarly to generating the initial dataset, each time after the control policy is improved, we sample N initial states, starting from which the safe control inputs in (12) are applied until arriving at the time horizon T . We add all the system transition data (totally NT data pairs) to the dataset \mathbf{D} . Then the FNN is retrained on the new dataset \mathbf{D} to minimize the loss function C in (7) (see Alg. 1).

Remark 1. The safe control u_t^s can only improve safety, rather than fully guarantee it, because: (1) bias exists between the learned model and the true model; (2) the error ϵ in $b(x_{t+1})$ is approximated by the first order derivative; (3) the error may exceed the lower limit. However, according to our simulation results (Section V), this method can significantly reduce the chance of the system reaching unsafe regions.

B. Control Policy Improvement

To solve (5) in Problem 1, we substitute the unknown system dynamics f with the learned one from Section IV-A. Also, we estimate the expected robustness over initial conditions by sampling M initial states x_0^1, \dots, x_0^M and averaging the resulting robustness values. For different initial states, different dropout masks Z_0^1, \dots, Z_0^M in the system model are sampled to estimate the trajectories. Along each trajectory the dropout mask is fixed. The average over initial conditions is also an average over samples of system model, hence it can reduce model-bias [21]. For brevity, let $\hat{f}^i(x_t, u_t) = x_t + \mathcal{F}(x_t, u_t; W_0, Z_0^i)$ denotes the sampled

Algorithm 1: System model learning

Input: A control policy π , a dataset \mathbf{D}
Output: Optimal FNN parameters W_0^*

```

1 if  $\mathbf{D}$  is empty then
2   for  $i \in 1, \dots, N_0$  do
3     Sample initial state  $x_0^i$ ;
4     for  $t \in 0, \dots, T-1$  do
5       Apply  $u_t^i \sim \text{Uniform}(\mathcal{U})$  to the system
        and add the data  $((x_t^i, u_t^i), \Delta_t^i)$  to  $\mathbf{D}$ ;
6       if close to unsafe area then
7         Break
8 else
9   for  $i \in 1, \dots, N$  do
10    Sample initial state  $x_0^i$ ;
11    for  $t \in 0, \dots, T-1$  do
12      Adjust  $\pi(x_{0:t}^i, W)$  to obtain  $u_t^{s,i}$  by (12);
13      Apply  $u_t^{s,i}$  to the system and add the data
         $((x_t^i, u_t^{s,i}), \Delta_t^i)$  to  $\mathbf{D}$ ;
14 Train the FNN on  $\mathbf{D}$ , return  $W_0^*$ ;

```

system model. Now the problem becomes:

$$W^* = \arg \max_W \frac{1}{M} \sum_{i=1}^M \rho(\varphi, x_{0:T}^i) \quad (13)$$

$$\text{s.t. } x_{t+1}^i = \hat{f}^i(x_t^i, \pi(x_{0:t}^i; W)),$$

$$t = 0, 1, \dots, T-1, i = 1, \dots, M.$$

One can solve (13) by substituting the constraints into the objective function and solve the unconstrained optimization problem. However, this is numerically unstable [11] because when computing the gradient of the objective function using the chain rule, the derivative calculated in the previous time step should be multiplied with the Jacobin matrix of the system model $\frac{\partial \hat{f}}{\partial x_t}$. If the eigenvalues of the Jacobian matrix are smaller than one, the gradients will vanish over time. If they are greater than one, the gradients will explode over time. To address this, we extended the Lagrange Multiplier method in [11] to RNN, which avoids the recursive multiplication of the gradients, and incrementally improves the robustness value.

We first consider only one trajectory starting from x_0 and the sampled system model is \hat{f} . By using Lagrange Multipliers, the system dynamics constraints can be incorporated into the objective function as:

$$\bar{J} = \rho(\varphi, x_{0:T}) + \sum_{t=0}^{T-1} \lambda_{t+1}^\top (\hat{f}(x_t, \pi(x_{0:t}; W)) - x_{t+1})$$

$$= \rho(\varphi, x_{0:T}) + H_0 - \lambda_T^\top x_T + \sum_{t=1}^{T-1} (H_t - \lambda_t^\top x_t), \quad (14)$$

where the Lagrange multipliers $\lambda_t \in \mathbb{R}^n$ are also called co-states and $H_t = \lambda_{t+1}^\top \hat{f}(x_t, \pi(x_{0:t}; W))$ is the Hamiltonian. The necessary condition for optimality is that the gradients of \bar{J} with respect to λ_t , x_t and W are all zero:

$$\frac{\partial \bar{J}}{\partial \lambda_{t+1}} = \hat{f}(x_t, \pi(x_{0:t}, W)) - x_{t+1} = 0, \quad t = 0, \dots, T-1, \quad (15)$$

$$\frac{\partial \bar{J}}{\partial x_t} = \frac{\partial \rho}{\partial x_t} + \sum_{j=0}^{T-1} \frac{\partial H_j}{\partial x_t} - \lambda_t = 0, \quad t = 1, \dots, T-1, \quad (16)$$

$$\frac{\partial \bar{J}}{\partial x_T} = \frac{\partial \rho}{\partial x_N} - \lambda_T = 0, \quad (17)$$

$$\frac{\partial \bar{J}}{\partial W} = \sum_{t=0}^{T-1} \frac{\partial H_t}{\partial W} = 0. \quad (18)$$

Solving (15) - (18) directly is difficult, so we apply an iteration method. At each optimization step, we force $\frac{\partial \bar{J}}{\partial \lambda_t}$ and $\frac{\partial \bar{J}}{\partial x_t}$ to be zero, i.e., (15) - (17) hold. Then we can compute the gradient $\frac{\partial \bar{J}}{\partial W}$ which is an ascent direction for \bar{J} . This procedure at each optimization step can be formulated as:

$$x_{t+1} = \hat{f}(x_t, \pi(x_{0:t}, W)), \quad t = 0, \dots, T-1, \quad (19)$$

$$\lambda_t = \frac{\partial \rho}{\partial x_t} + \sum_{j=t+1}^{T-1} \lambda_{j+1} \frac{\partial \hat{f}}{\partial u_j} \frac{\partial u_j}{\partial x_t} \quad (20)$$

$$+ \lambda_{t+1} \left(\frac{\partial \hat{f}}{\partial x_t} + \frac{\partial \hat{f}}{\partial u_t} \frac{\partial u_t}{\partial x_t} \right), \quad t = 1, \dots, T-1, \quad (21)$$

$$\frac{\partial \bar{J}}{\partial W} = \sum_{t=0}^{T-1} \lambda_{t+1} \frac{\partial \hat{f}}{\partial u_t} \frac{\partial u_t}{\partial W}. \quad (22)$$

Equations (19) - (22) are derived from (15) - (18) respectively. At each optimization step, we use (19) - (21) to compute x_t and λ_t , and substitute them into (22) to compute $\frac{\partial \bar{J}}{\partial W}$. This is the gradient for one trajectory. We denote $\frac{\partial \bar{J}}{\partial W}$ for the trajectory starting from x_0^i by δW^i . The gradient of the objective function in (13) with respect to W can be computed by:

$$\Delta W = \frac{1}{M} \sum_{i=1}^M \delta W^i. \quad (23)$$

At each optimization step, we compute the gradient ΔW and use the optimization method Adam [31] to update the policy parameters W until convergence. Then the optimal policy parameters W^* is found. The policy improvement process is shown in Alg. 2.

Remark 2. All the derivatives involving the FNN system model and the RNN controller ($\frac{\partial \hat{f}}{\partial u}$, $\frac{\partial \hat{f}}{\partial x}$, $\frac{\partial u}{\partial x}$, $\frac{\partial u}{\partial W}$) can be computed automatically and analytically by using the auto-differentiation tools designed for neural networks (e.g., PyTorch [32]). For the derivatives of the STL robustness ρ , we applied the method STLCG [25], which computes the robustness value using a computation graph similar to a neural network. So the auto-differentiation tools can also be applied to compute $\frac{\partial \rho}{\partial x}$. Hence, all the derivatives in (19) - (22) can be accessed easily and analytically.

Algorithm 2: Control policy improvement

Input: A learned model \hat{f} , an STL formula φ

Output: Optimal policy parameters W^*

```

1 repeat
2   for  $i \in 1, \dots, M$  do
3     Sample initial state  $x_0^i$  and system model  $\hat{f}^i$ ;
4     Compute  $\delta W_i$  by Equations (19) - (22);
5   end
6   Compute  $\Delta W$  by Equation (23);
7   Update  $W$  using the Adam optimizer;
8 until Convergence; return  $W^*$ ;
9 3

```

Algorithm 3: Model-based policy search

Input: An STL formula φ

Output: Optimal policy parameters W^*

```

1 Initialize  $W_0$ ,  $W$ , and an empty dataset  $\mathbf{D}$ ;
2 repeat
3   Train the system model using Algorithm 1;
4   Train the controller using Algorithm 2;
5 until convergence; return  $W^*$ ;

```

C. Model-based policy search

We alternately use Alg. 1 and Alg. 2 to train the system model and the control policy. We call the completion of one model learning and one policy improvement a *cycle*. The algorithm will terminate and return the final control policy with parameter W^* when the policy converges. The overall model-based policy search method is shown in Alg. 3.

V. CASE STUDIES

In this section, we evaluate our approach on two case studies. We compare the results with the approach in [12], where an RNN controller is trained via imitation learning, i.e., a dataset containing success trajectories is first generated and the controller is trained on that dataset. The system dynamics in [12] are assumed to be known.

All algorithms developed in this paper were implemented in Python. The RNN was implemented using Pytorch [32]. We used a Mac with a 2.6GHz Core i7 CPU and 16GB of RAM for both the method developed in this paper and for the one from [12].

A. Case Study I

We consider a discrete time unicycle robot in a 2-dimensional environment with dynamics:

$$\begin{aligned} p_{x,t+1} &= p_{x,t} + \frac{v_t}{\omega_t} (\sin(\theta_t + \omega_t) - \sin \theta_t), \\ p_{y,t+1} &= p_{y,t} + \frac{v_t}{\omega_t} (\cos \theta_t - \cos(\theta_t + \omega_t)), \\ \theta_{t+1} &= \theta_t + \omega_t. \end{aligned} \quad (24)$$

The system state $x = [p_x \ p_y \ \theta]^\top$ gives the position and orientation of the robot. The control input $u = [v \ \omega]^\top$ captures the speed and angular speed, with $v \in [0, 0.75]$ and

$\omega \in [-\frac{\pi}{2}, \frac{\pi}{2}]$. The initial state x_0 is uniformly distributed in \mathcal{X}_0 , i.e., $x_0 \sim \text{Uniform}(\mathcal{X}_0)$, where $\mathcal{X}_0 = [0.5, 2] \times [0.5, 2]$.

Following the procedure from this paper, we assume that the robot dynamics are not known. We use the system dynamics (24) as a proxy for the real robot, since we do not run real experiments in this paper. Specifically, we use dynamics (24) to collect system transition data to train the system model, and to test the obtained control policy. When collecting data, we add a random noise $w_t \in [-0.1, 0.1]^3$ to the observed state x_t to simulate a real world situation.

The specification is to “eventually visit *RegA* or *RegB* within $[0, 10]$ and eventually visit *RegC* within $[11, 20]$ and always avoid *Obs*”. This can be written as an STL formula:

$$\varphi_1 = (\mathbf{F}_{[0,10]}(\text{RegA} \vee \text{RegB})) \wedge (\mathbf{F}_{[11,20]}\text{RegC}) \wedge (\mathbf{G}_{[0,20]}\neg\text{Obs}), \quad (25)$$

where we assumed that the final time is 20, which is also the time horizon of φ_1 . The regions are shown in Fig. 3. The safety requirement is to avoid the round obstacle *Obs*. When generating the initial dataset, we stop the system if the distance between the robot and the obstacle is less than 0.75 (the maximum moving distance in one step). After that, safety is guaranteed by a CBF:

$$b(x_t) = (p_{x,t} - c_x)^2 + (p_{y,t} - c_y)^2 - r^2, \quad (26)$$

where (c_x, c_y) is the center of the obstacle and r is the radius.

When training the model, we collect $N_0 = 10$ trajectories in the initial dataset, and each time after the policy is improved, we add $N = 3$ trajectories. When training the policy, we sample $M = 4$ initial states. Let $\alpha = 0.7$ in (12). When computing the norm in (12) we assign a weight of 0.01 to the angular speed in order to encourage the robot to turn instead of slowing down when approaching an obstacle. The RNN applies an LSTM [33] containing 2 hidden layers each with 32 nodes. The FNN has 2 hidden layers each with 32 nodes and the dropout probability $p_d = 0.1$.

The next step is to search for the optimal control policy. The approximated expectation of robustness $\frac{1}{M} \sum_{i=1}^M \rho(\varphi, x_{0:T}^i)$ during the entire training process is shown in Fig 2. The vertical lines show when the system model is updated. Fig. 3 shows the testing results of the trained policy after each cycle. The control inputs given by the policy are adjusted (if necessary) using CBF to improve safety. The success rate γ (obtaining trajectories with positive robustness) is evaluated on 1000 trajectories. Note that although 10 trajectories are plotted in the figures, only $N = 3$ trajectories are added to the dataset after each cycle. We can see that after updating the model the policy can be improved to get a higher robustness. The resulting success rate increases as well. This shows that a better model benefits the policy improvement. After 6 cycles, the success rate reaches 100%. In the entire training process, the system runs for a total of $N_0 + 5N = 25$ times. This shows that our algorithm can learn a policy that fully satisfies the given specification with relatively few system executions.

In Fig. 3a, one of the trajectories goes into the obstacle region (although in practice we only collect $N = 3$ tra-

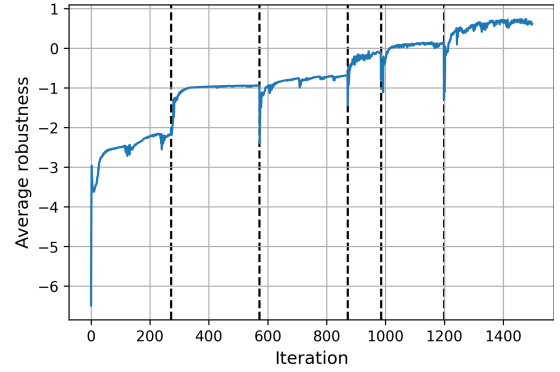


Fig. 2: The average robustness for φ_1 during the training process. Vertical dash lines indicate when the system model is updated.

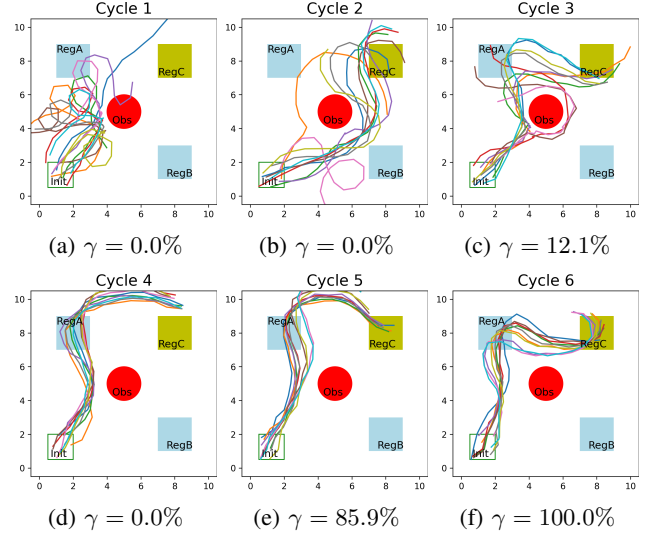


Fig. 3: Testing results of the control policy after each cycle. The controls are adjusted using CBF. In each figure 10 trajectories are plotted. The success rate γ is evaluated on 1000 trajectories.

jectories and no violations of safety are observed). With the improvement of the model and the policy, no more violations occur. We take the model and the policy after the third cycle as an example to illustrate the efficacy of our CBF-based safe control method. We generate trajectories with and without CBF and compare them in Fig. 4. When not using CBF (Fig. 4a), we can see that many trajectories go through the obstacle. After CBF is applied (Fig. 4b), the trajectories go around the obstacle. Although safety is not 100% guaranteed, using CBF can significantly improve the safety performance.

As stated at the beginning of this section, we compare the approach in this paper with our previous work [12], in which the model is assumed to be known and an RNN controller is trained on a dataset containing satisfying trajectories. Using the method from [12], it takes more than 2 hours to obtain a controller that can finish the same task as above and the success rate is 99%. By contrast, in our new approach training the model and the policy for 6 cycles takes about 50 minutes and the success rate reaches 100%. The explanation is that in [12], a lot of time (2 hours) is spent on generating the dataset, while in our new approach we directly search

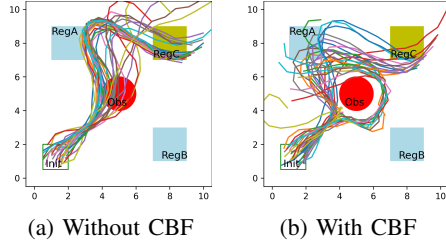


Fig. 4: Trajectories generated with and without CBF after 3 cycles of training. 30 trajectories are shown in each figure.

the policy to improve the robustness.

After training, the control policy (RNN controller) can be implemented very fast. In this paper, it takes about 0.0004s to obtain the control input at each state. With a well-trained policy, the CBF constraint in (12) is easy to satisfy, so solving (12) is also very fast (takes about 0.01s in this case), which suggests that it can be implemented in real time.

B. Case Study II

In this example, we consider a system given by:

$$\begin{aligned} p_{x,t+1} &= p_{x,t} + v_{x,t} \\ p_{y,t+1} &= p_{y,t} + v_{y,t}, \end{aligned} \quad (27)$$

where the system state $x = [p_x \ p_y]^\top$ gives the x-y position of a robot and the control input $u = [v_x \ v_y]^\top$ captures the velocity with $u \in [-2, 2]^2$. Again, the system dynamics (27) are assumed to be unknown and we add a random noise $w_t \in [-0.1, 0.1]^2$ to the observed state x_t .

The specification is: “for all $t \in [0, 15]$, eventually visit *RegA* every $[t, t+7]$ and eventually visit *RegB* every $[t, t+7]$, and always stay in the *Safe* region”, which translates to the STL formula:

$$\varphi_2 = \mathbf{G}_{[0,15]}(\mathbf{F}_{[0,7]} \text{RegA} \wedge \mathbf{F}_{[0,7]} \text{RegB}) \wedge \mathbf{G}_{[0,22]} \text{Safe}. \quad (28)$$

The regions are shown in Fig. 5, where the interior of the disk is the *Safe* region. The time horizon of φ_2 is 22, which is also our planning horizon.

The safety requirement is to stay in the *Safe* region. When generating the initial dataset, we stop the system if the distance between the robot and the boundary of the safe region is less than $2\sqrt{2}$ (maximum moving distance in one step). In the following cycles, we guarantee safety by a CBF:

$$b(x_t) = r^2 - (p_{x,t} - c_x)^2 - (p_{y,t} - c_y)^2, \quad (29)$$

where (c_x, c_y) is the center of the *Safe* region, r is its radius.

Let $N_0 = 10$, $N = 6$, $\alpha = 0.98$, $p_d = 0.05$. The other settings are the same as the ones from the first case study. In this case, the robot has to move back and forth between *RegA* and *RegB* in order to satisfy the specification. When between the two regions, the robot needs to know which region it has just visited so that it can move towards the other one. Hence, it is impossible for a control policy that only depends on the current state to accomplish this task. To illustrate that this *history-dependence* problem can be solved by an RNN controller, we trained another policy using the approach in this paper, but the policy is implemented by an

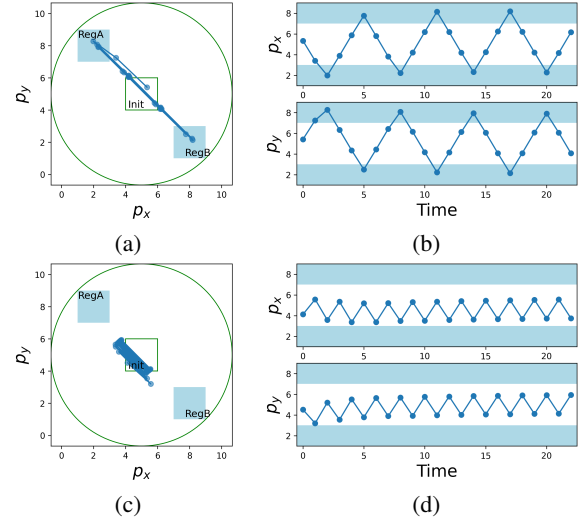


Fig. 5: (a), (b) show a trajectory generated by an RNN controller. (c), (d) show a trajectory generated by an FNN controller.

FNN rather than an RNN. The FNN controller has 2 hidden layers each with 32 nodes. We compare two sample trajectories, one from the RNN controller and the other from the FNN controller in Fig. 5. We can see that at the same location (between the two regions), the RNN controller can output different controls depending on the history trajectories, so the robot can move back and forth between the two regions and successfully satisfy the specification. On the other hand, the FNN controller can only output the same controls at the same location, hence the robot oscillates near the initial location and fails to finish this task.

Next, we visualize the training process of the RNN control policy. The approximated expectation of robustness during training is shown in Fig. 6. We sample 20 trajectories using the policy after each cycle (shown in Fig. 7). Similar to Case Study I, the policy is improved after each cycle of training. The success rate reaches 100.0% after 4 cycles, which takes about 25 minutes. In contrast, the approach in [12] takes more than 40 minutes to finish a related, simpler task. The system is executed for $N_0 + 3N = 28$ times during training. The learned policy takes about 0.0004s to compute the control at each state. This again proves that our approach has the potential to be used on real world systems and for real time control.

VI. CONCLUSION

In this paper, we proposed a model-based policy search approach to satisfy specifications given as STL formulae. The system model and the control policy are learned alternately. The policy is implemented as an RNN, which can deal with the history-dependence property of STL. The simulation results show that our approach can learn the control policy within few system executions and achieves high success rate. Safety can be significantly improved by using CBFs. After training, the RNN policy can output controls very fast, which enables real time implementation.

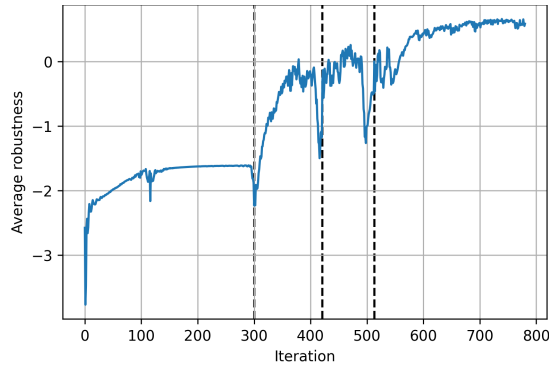


Fig. 6: The average robustness for φ_2 during the training process. Vertical dash lines indicate when the system model is updated.

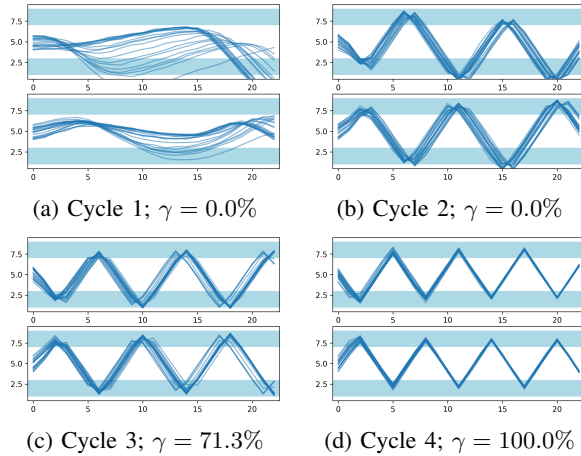


Fig. 7: Testing results of the control policy after each cycle. The controls are adjusted using the CBF. In each figure 20 trajectories are plotted. The success rate γ is evaluated on 1000 trajectories.

REFERENCES

- [1] C. Baier and J.-P. Katoen, *Principles of model checking*. MIT press, 2008.
- [2] O. Maler and D. Nickovic, "Monitoring temporal properties of continuous signals," in *Formal Techniques, Modelling and Analysis of Timed and Fault-Tolerant Systems*. Springer, 2004, pp. 152–166.
- [3] A. Donzé and O. Maler, "Robust satisfaction of temporal logic over real-valued signals," in *International Conference on Formal Modeling and Analysis of Timed Systems*. Springer, 2010, pp. 92–106.
- [4] V. Raman, A. Donzé, M. Maasoumy, R. M. Murray, A. Sangiovanni-Vincentelli, and S. A. Seshia, "Model predictive control with signal temporal logic specifications," in *53rd IEEE Conference on Decision and Control*. IEEE, 2014, pp. 81–87.
- [5] S. Sadraddini and C. Belta, "Robust temporal logic model predictive control," in *2015 53rd Annual Allerton Conference on Communication, Control, and Computing (Allerton)*. IEEE, 2015, pp. 772–779.
- [6] Y. V. Pant, H. Abbas, and R. Mangharam, "Smooth operator: Control using the smooth robustness of temporal logic," in *2017 IEEE Conference on Control Technology and Applications (CCTA)*. IEEE, 2017, pp. 1235–1240.
- [7] I. Haghighi, N. Mehdipour, E. Bartocci, and C. Belta, "Control from signal temporal logic specifications with smooth cumulative quantitative semantics," in *2019 IEEE 58th Conference on Decision and Control (CDC)*. IEEE, 2019, pp. 4361–4366.
- [8] N. Mehdipour, C.-I. Vasile, and C. Belta, "Arithmetic-geometric mean robustness for control from signal temporal logic specifications," in *2019 American Control Conference (ACC)*. IEEE, 2019, pp. 1690–1695.
- [9] P. Varnai and D. V. Dimarogonas, "On robustness metrics for learning stl tasks," in *2020 American Control Conference (ACC)*. IEEE, 2020, pp. 5394–5399.
- [10] Y. Gilpin, V. Kurtz, and H. Lin, "A smooth robustness measure of signal temporal logic for symbolic control," *IEEE Control Systems Letters*, vol. 5, no. 1, pp. 241–246, 2020.
- [11] S. Yaghoubi and G. Fainekos, "Worst-case satisfaction of stl specifications using feedforward neural network controllers: a lagrange multipliers approach," in *2020 Information Theory and Applications Workshop (ITA)*. IEEE, 2020, pp. 1–20.
- [12] W. Liu, N. Mehdipour, and C. Belta, "Recurrent neural network controllers for signal temporal logic specifications subject to safety constraints," *IEEE Control Systems Letters*, 2021.
- [13] D. Amodi, C. Olah, J. Steinhardt, P. Christiano, J. Schulman, and D. Mané, "Concrete problems in ai safety," *arXiv preprint arXiv:1606.06565*, 2016.
- [14] D. Aksaray, A. Jones, Z. Kong, M. Schwager, and C. Belta, "Q-learning for robust satisfaction of signal temporal logic specifications," in *2016 IEEE 55th Conference on Decision and Control (CDC)*. IEEE, 2016, pp. 6565–6570.
- [15] H. Venkataraman, D. Aksaray, and P. Seiler, "Tractable reinforcement learning of signal temporal logic objectives," in *Learning for Dynamics and Control*. PMLR, 2020, pp. 308–317.
- [16] A. Balakrishnan and J. V. Deshmukh, "Structured reward shaping using signal temporal logic specifications," in *2019 IEEE/RSJ International Conference on Intelligent Robots and Systems (IROS)*. IEEE, 2019, pp. 3481–3486.
- [17] X. Li, C.-I. Vasile, and C. Belta, "Reinforcement learning with temporal logic rewards," in *2017 IEEE/RSJ International Conference on Intelligent Robots and Systems (IROS)*. IEEE, 2017, pp. 3834–3839.
- [18] X. Li, Y. Ma, and C. Belta, "A policy search method for temporal logic specified reinforcement learning tasks," in *2018 Annual American Control Conference (ACC)*. IEEE, 2018, pp. 240–245.
- [19] P. Varnai and D. V. Dimarogonas, "Prescribed performance control guided policy improvement for satisfying signal temporal logic tasks," in *2019 American Control Conference (ACC)*. IEEE, 2019, pp. 286–291.
- [20] X. Li, Z. Serlin, G. Yang, and C. Belta, "A formal methods approach to interpretable reinforcement learning for robotic planning," *Science Robotics*, vol. 4, no. 37, 2019.
- [21] M. Deisenroth and C. E. Rasmussen, "Pilco: A model-based and data-efficient approach to policy search," in *Proceedings of the 28th International Conference on machine learning (ICML-11)*. Citeseer, 2011, pp. 465–472.
- [22] Y. Gal, R. McAllister, and C. E. Rasmussen, "Improving pilco with bayesian neural network dynamics models," in *Data-Efficient Machine Learning workshop, ICML*, vol. 4, no. 34, 2016, p. 25.
- [23] P. Kapoor, A. Balakrishnan, and J. V. Deshmukh, "Model-based reinforcement learning from signal temporal logic specifications," *arXiv preprint arXiv:2011.04950*, 2020.
- [24] Y. Gal and Z. Ghahramani, "Dropout as a bayesian approximation: Representing model uncertainty in deep learning," in *international conference on machine learning*. PMLR, 2016, pp. 1050–1059.
- [25] K. Leung, N. Archéga, and M. Pavone, "Back-propagation through signal temporal logic specifications: Infusing logical structure into gradient-based methods," *arXiv preprint arXiv:2008.00097*, 2020.
- [26] A. D. Ames, S. Coogan, M. Egerstedt, G. Notomista, K. Sreenath, and P. Tabuada, "Control barrier functions: Theory and applications," in *2019 18th European Control Conference (ECC)*. IEEE, 2019, pp. 3420–3431.
- [27] A. Dokhanchi, B. Hoxha, and G. Fainekos, "On-line monitoring for temporal logic robustness," in *International Conference on Runtime Verification*. Springer, 2014, pp. 231–246.
- [28] I. Goodfellow, Y. Bengio, and A. Courville, *Deep learning*, 2016, vol. 1, no. 2.
- [29] A. Agrawal and K. Sreenath, "Discrete control barrier functions for safety-critical control of discrete systems with application to bipedal robot navigation," in *Robotics: Science and Systems*, 2017.
- [30] D. P. Bertsekas, "Nonlinear programming," *Journal of the Operational Research Society*, vol. 48, no. 3, pp. 334–334, 1997.
- [31] D. P. Kingma and J. Ba, "Adam: A method for stochastic optimization," *arXiv preprint arXiv:1412.6980*, 2014.
- [32] A. Paszke, S. Gross, S. Chintala, G. Chanan, E. Yang, Z. DeVito, Z. Lin, A. Desmaison, L. Antiga, and A. Lerer, "Automatic differentiation in pytorch," 2017.
- [33] S. Hochreiter and J. Schmidhuber, "Long short-term memory," *Neural computation*, vol. 9, no. 8, pp. 1735–1780, 1997.